

QCM-SGM+: Improved Quantized Compressed Sensing With Score-Based Generative Models for General Sensing Matrices

Xiangming Meng¹ Yoshiyuki Kabashima¹

Abstract

In realistic compressed sensing (CS) scenarios, the obtained measurements usually have to be quantized to a finite number of bits before transmission and/or storage, thus posing a challenge in recovery, especially for extremely coarse quantization such as 1-bit sign measurements. Recently Meng & Kabashima (2023) proposed an efficient quantized compressed sensing algorithm called QCS-SGM using the score-based generative models as an implicit prior. Thanks to the power of score-based generative models in capturing the rich structure of the prior, QCS-SGM achieves remarkably better performances than previous quantized CS methods. However, QCS-SGM is restricted to (approximately) row-orthogonal sensing matrices since otherwise the likelihood score becomes intractable. To address this challenging problem, in this paper we propose an improved version of QCS-SGM, which we call QCS-SGM+, which also works well for general matrices. The key idea is a Bayesian inference perspective of the likelihood score computation, whereby an expectation propagation algorithm is proposed to approximately compute the likelihood score. Experiments on a variety of baseline datasets demonstrate that the proposed QCS-SGM+ outperforms QCS-SGM by a large margin when sensing matrices are far from row-orthogonal.

1. Introduction

In this paper, we consider the nonlinear inverse problem from noisy quantized measurements as follows (Zymnis et al., 2009)

$$\mathbf{y} = \mathbf{Q}(\mathbf{Ax} + \mathbf{n}), \quad (1)$$

¹Institute for Physics of Intelligence and Department of Physics, The University of Tokyo, Japan. Correspondence to: Xiangming Meng <meng@g.ecc.u-tokyo.ac.jp>.

where the goal is to recover the unknown signal $\mathbf{x} \in \mathbb{R}^{N \times 1}$ from quantized measurements $\mathbf{y} \in \mathbb{R}^{M \times 1}$, where $\mathbf{A} \in \mathbb{R}^{M \times N}$ is a known linear mixing matrix, $\mathbf{n} \sim \mathcal{N}(\mathbf{n}; 0, \sigma^2 \mathbf{I})$ is an i.i.d. additive Gaussian noise, and $\mathbf{Q}(\cdot) : \mathbb{R}^{M \times 1} \rightarrow \mathcal{Q}^{M \times 1}$ is an *element-wise* quantizer function which maps each element into a finite (or countable) set of codewords \mathcal{Q} , i.e., $y_m = \mathbf{Q}(z_m + n_m) \in \mathcal{Q}$, or equivalently $(z_m + n_m) \in \mathbf{Q}^{-1}(y_m)$, $m = 1, 2, \dots, M$, where z_m is the m -th element of $\mathbf{z} = \mathbf{Ax}$. Same as Meng & Kabashima (2023), we consider the uniform quantizer with Q quantization bits (resolution) and a quantization interval $\Delta > 0$. The quantization codewords $\mathcal{Q} = \{q_r\}_{r=1}^{2^Q}$ consist of 2^Q elements, i.e.,

$$q_r = (2r - 2^Q - 1) \Delta / 2, \quad r = 1, \dots, 2^Q, \quad (2)$$

where the lower and upper thresholds associated with q_r are

$$l_{q_r} = \begin{cases} -\infty, r = 1; \\ (r - 2^{Q-1} - 1) \Delta, r = 2, \dots, 2^Q. \end{cases} \quad (3)$$

$$u_{q_r} = \begin{cases} (r - 2^{Q-1}) \Delta, r = 1, \dots, 2^Q - 1; \\ +\infty, r = 2^Q. \end{cases} \quad (4)$$

In other words, $\mathbf{Q}^{-1}(q_r) = [l_{q_r}, u_{q_r}]$ or equivalently, $l_{q_r} \leq \mathbf{Q}^{-1}(q_r) < u_{q_r}$. In the extreme 1-bit case, i.e., $Q = 1$, only the sign values are observed, i.e.,

$$\mathbf{y} = \text{sign}(\mathbf{Ax} + \mathbf{n}), \quad (5)$$

where the quantization codewords $\mathcal{Q} = \{-1, +1\}$.

This problem, widely known as quantized compressed sensing (CS), is ubiquitous in various applications due to the fact that in realistic acquisition scenarios, the obtained measurements have to be quantized to a finite number of Q bits before transmission and/or storage (Zymnis et al., 2009; Dai & Milenkovic, 2011). Inevitably, the quantization process leads to information loss which makes the recovery particularly challenging. As a result, a naive application of traditional CS methods by ignoring the quantization is suboptimal (Dai & Milenkovic, 2011), especially for the extreme 1-bit case. As a result, there has been an extensive study of algorithms specially designed for quantized CS by explicitly taking into account the quantization operation

(Zymnis et al., 2009; Dai & Milenkovic, 2011; Plan & Vershynin, 2012; 2013; Jacques et al., 2013; Xu & Kabashima, 2013; Xu et al., 2014; Awasthi et al., 2016; Meng et al., 2018; Jung et al., 2021; Liu et al., 2020; Liu & Liu, 2022; Zhu et al., 2022). Among various quantized CS algorithms, one key design factor is the prior distribution of unknown signal \mathbf{x} since it represents our prior knowledge of the target. Apparently, the more we know about the target, the less we need to recover it, which is also the case under the quantized scenario. As a result, while the sparsity, whether naive sparsity or structured sparsity, is the most popular prior assumption used in CS, it is too simple to capture the rich structure inherent in natural signals. In turn, one has to acquire a larger number of observations to accurately recover the desired signal.

Recently, with the advent of deep generative models (Goodfellow et al., 2014; Kingma & Welling, 2013; Rezende & Mohamed, 2015; Song & Ermon, 2019; 2020; Sohl-Dickstein et al., 2015; Ho et al., 2020; Nichol & Dhariwal, 2021) in density estimation, there has been a surge of interests in developing CS algorithms with data-driven priors (Bora et al., 2017; Hand & Joshi, 2019; Asim et al., 2020; Pan et al., 2021), i.e., the prior $p(\mathbf{x})$ of \mathbf{x} is learned, either explicitly or implicitly, through a generative model, such as VAE (Kingma & Welling, 2013) GAN (Goodfellow et al., 2014), and the most recent score-based generative models (SGM) or diffusion models (DM) (Song & Ermon, 2019; 2020; Sohl-Dickstein et al., 2015; Ho et al., 2020; Nichol & Dhariwal, 2021). Due to the powerful representation capability of deep generative models, one is armed with much better knowledge of the target signal than the hand-crafted prior such as sparsity, and therefore requires much fewer measurements in signal recovery. Notably, Meng & Kabashima (2023) proposed an efficient algorithm called QCS-SGM based on SGM (Song & Ermon, 2019; 2020) using score matching with Langevin dynamics (SMLD) (Song & Ermon, 2019; 2020) and achieves the state-of-the-art (SOTA) performances for quantized CS. Nevertheless, QCS-SGM builds on a strong assumption that the sensing matrix \mathbf{A} is (approximately) row-orthogonal. Otherwise, the likelihood score becomes intractable and QCS-SGM will degrade apparently due to such inaccurate score approximation, which severely limits the application of QCS-SGM (Meng & Kabashima, 2023) for more general sensing matrices.

In this paper, we address the limitation of QCS-SGM by extending it to general sensing matrices. The main contributions are summarized as follows.

1.1. Contributions

- We propose an improved version of QCS-SGM, which we call QCS-SGM+, which works well for general

matrices. The key idea is a Bayesian inference perspective of the likelihood score computation, i.e., the computation of the likelihood score can be viewed as a Bayesian inference problem and thus approximate inference method can be applied to yield approximate solutions. In particular, by resorting to the famous expectation propagation (Minka, 2001), we obtain an efficient approximation of the likelihood score which is more accurate than QCS-SGM when sensing matrices are no longer row-orthogonal.

- We verify the effectiveness of the proposed QCS-SGM+ in QCS on various real-world datasets including MNIST, Cifar-10, CelebA 64×64 . Using the pre-trained SGM as a generative prior, the proposed QCS-SGM+ outperforms QCS-SGM and other quantized CS algorithms by a large margin when the sensing matrix is far from row-orthogonal.

1.2. Related works

Generative Models for CS: This line of research learns a generative prior from data which is then used for inference (Jin et al., 2017; Bora et al., 2017; Hand & Joshi, 2019; Asim et al., 2020; Pan et al., 2021; Meng & Kabashima, 2022). Most studies follow the classic CSGM framework (Jin et al., 2017), and the difference lies in the generative models used, e.g., VAE (Kingma & Welling, 2013), GAN (Goodfellow et al., 2014), SGM or DM (Song & Ermon, 2019; 2020; Sohl-Dickstein et al., 2015; Ho et al., 2020; Nichol & Dhariwal, 2021). Note that both VAE and GAN might have large representation errors or biases due to inappropriate latent dimensionality and/or mode collapse (Asim et al., 2020). Moreover, GAN suffers from unstable training due to the adversarial training nature while VAE uses a surrogate loss. By contrast, SGM or DM (Song & Ermon, 2019; 2020; Ho et al., 2020; Nichol & Dhariwal, 2021) have proven extremely effective and even outperform the state-of-the-art (SOTA) GAN (Goodfellow et al., 2014) and VAE (Kingma & Welling, 2013) in density estimation and generation of various natural sources such as images and audios (Dhariwal & Nichol, 2021; Rombach et al., 2022).

Generative Models for quantized CS: Recent works Liu et al. (2020); Liu & Liu (2022) extended CSGM framework to non-linear observations including 1-bit CS. However, the main focuses of Liu et al. (2020); Liu & Liu (2022) are limited to VAE and GAN (in particular DCGAN (Radford et al., 2015)), and thus inherit the disadvantages of VAE and GAN. In the very recent work Meng & Kabashima (2023), the authors proposed a novel algorithm QCS-SGM by resorting to SGM or DM as an implicit prior, which achieves state-of-the-art (SOTA) performances for quantized CS. Unfortunately, QCS-SGM is strictly restricted to row-orthogonal sensing matrices.

2. Background

2.1. Score-based Generative Models

For any continuously differentiable probability density function $p(\mathbf{x})$, if we have access to its score function, i.e., $\nabla_{\mathbf{x}} \log p(\mathbf{x})$, we can iteratively sample from it using Langevin dynamics (Turq et al., 1977; Bussi & Parrinello, 2007; Welling & Teh, 2011)

$$\mathbf{x}_t = \mathbf{x}_{t-1} + \alpha_t \nabla_{\mathbf{x}_{t-1}} \log p(\mathbf{x}_{t-1}) + \sqrt{2\alpha_t} \mathbf{z}_t, \quad 1 \leq t \leq T, \quad (6)$$

where $\mathbf{z}_t \sim \mathcal{N}(\mathbf{z}_t; \mathbf{0}, \mathbf{I})$, $\alpha_t > 0$ is the step size, and T is the total number of iterations. It has been demonstrated that when α_t is sufficiently small and T is sufficiently large, the distribution of \mathbf{x}_T will converge to $p(\mathbf{x})$ (Roberts & Tweedie, 1996; Welling & Teh, 2011). In practice, the score function $\nabla_{\mathbf{x}} \log p(\mathbf{x})$ is unknown and can be estimated using a *score network* $s_{\theta}(\mathbf{x})$ via score matching (Hyvärinen, 2006; Vincent, 2011). However, the vanilla Langevin dynamics faces a variety of challenges such as slow convergence. To address this challenge, inspired by simulated annealing (Kirkpatrick et al., 1983; Neal, 2001), Song & Ermon (2019) proposed an annealed version of Langevin dynamics, which perturbs the data with Gaussian noise of different scales and jointly estimates the score functions of noise-perturbed data distributions. Accordingly, during the inference, an annealed Langevin dynamics (ALD) is performed to leverage the information from all noise scales.

Specifically, assume that $p_{\beta}(\tilde{\mathbf{x}} | \mathbf{x}) = \mathcal{N}(\tilde{\mathbf{x}}; \mathbf{x}, \beta^2 \mathbf{I})$, and so we have $p_{\beta}(\tilde{\mathbf{x}}) = \int p_{\text{data}}(\mathbf{x}) p_{\beta}(\tilde{\mathbf{x}} | \mathbf{x}) d\mathbf{x}$, where $p_{\text{data}}(\mathbf{x})$ is the data distribution. Consider we have a sequence of noise scales $\{\beta_t\}_{t=1}^T$ satisfying $\beta_{\max} = \beta_1 > \beta_2 > \dots > \beta_T = \beta_{\min} > 0$. The $\beta_{\min} \rightarrow 0$ is small enough so that $p_{\beta_{\min}}(\tilde{\mathbf{x}}) \approx p_{\text{data}}(\mathbf{x})$, and β_{\max} is large enough so that $p_{\beta_{\max}}(\tilde{\mathbf{x}}) \approx \mathcal{N}(\mathbf{x}; \mathbf{0}, \beta_{\max}^2 \mathbf{I})$. The noise conditional score network (NCSN) $s_{\theta}(\mathbf{x}, \beta)$ proposed in Song & Ermon (2019) aims to estimate the score function of each $p_{\beta_t}(\tilde{\mathbf{x}})$ by optimizing the following weighted sum of score matching objective

$$\theta^* = \arg \min_{\theta} \sum_{t=1}^T \mathbb{E}_{p_{\text{data}}(\mathbf{x})} \mathbb{E}_{p_{\beta_t}(\tilde{\mathbf{x}} | \mathbf{x})} \left[\|s_{\theta}(\tilde{\mathbf{x}}, \beta_t) - \nabla_{\tilde{\mathbf{x}}} \log p_{\beta_t}(\tilde{\mathbf{x}} | \mathbf{x})\|_2^2 \right]. \quad (7)$$

After training the NCSN, for each noise scale, we can run K steps of Langevin MCMC to obtain a sample for each $p_{\beta_t}(\tilde{\mathbf{x}})$ as

$$\mathbf{x}_t^k = \mathbf{x}_t^{k-1} + \alpha_t s_{\theta}(\mathbf{x}_t^{k-1}, \beta_t) + \sqrt{2\alpha_t} \mathbf{z}_t^k, \quad k = 1, \dots, K. \quad (8)$$

The sampling process is repeated for $t = 1, 2, \dots, T$ sequentially with $\mathbf{x}_1^0 \sim \mathcal{N}(\mathbf{x}; \mathbf{0}, \beta_{\max}^2 \mathbf{I})$ and $\mathbf{x}_{t+1}^0 = \mathbf{x}_t^K$ when

$t < T$. As shown in Song & Ermon (2019), when $K \rightarrow \infty$ and $\alpha_t \rightarrow 0$ for all t , the final sample \mathbf{x}_T^K will become an exact sample from $p_{\beta_{\min}}(\tilde{\mathbf{x}}) \approx p_{\text{data}}(\mathbf{x})$ under some regularity conditions. Later, by a theoretical analysis of the learning and sampling process of NCSN, an improved version of NCSN, termed NCSNv2, was proposed in Song & Ermon (2020) which is more stable and can scale to various datasets with high resolutions.

2.2. QCS-SGM: Quantized CS with SGM

Recently, Meng & Kabashima (2023) proposed an efficient method called QCS-SGM for quantized CS using SGM as implicit prior. The basic idea is that, in the case of quantized measurements (1), to sample from the posterior distribution $p(\mathbf{x} | \mathbf{y})$ rather than $p(\mathbf{x})$, the Langevin dynamics in (6) becomes

$$\mathbf{x}_t = \mathbf{x}_{t-1} + \alpha_t \nabla_{\mathbf{x}_{t-1}} \log p(\mathbf{x}_{t-1} | \mathbf{y}) + \sqrt{2\alpha_t} \mathbf{z}_t, \quad 1 \leq t \leq T, \quad (9)$$

where the conditional (*posterior*) score $\nabla_{\mathbf{x}} \log p(\mathbf{x} | \mathbf{y})$ is required. Using the Bayesian rule, the $\nabla_{\mathbf{x}_t} \log p(\mathbf{x}_t | \mathbf{y})$ is decomposed into two terms

$$\nabla_{\mathbf{x}_t} \log p(\mathbf{x}_t | \mathbf{y}) = \nabla_{\mathbf{x}_t} \log p(\mathbf{x}_t) + \nabla_{\mathbf{x}_t} \log p(\mathbf{y} | \mathbf{x}_t), \quad (10)$$

which include the unconditional score $\nabla_{\mathbf{x}_t} \log p(\mathbf{x}_t)$ (termed as *prior score* in Meng & Kabashima (2023)), and the conditional score $\nabla_{\mathbf{x}_t} \log p(\mathbf{y} | \mathbf{x}_t)$ (termed as *likelihood score* in Meng & Kabashima (2023)), respectively. While the prior score $\nabla_{\mathbf{x}_t} \log p(\mathbf{x}_t)$ can be easily obtained using a trained score network such as NCSN or NCSNv2, the likelihood score $\nabla_{\mathbf{x}_t} \log p(\mathbf{y} | \mathbf{x}_t)$ is generally intractable. To tackle this difficulty, Meng & Kabashima (2023) proposed a simple yet effective approximation of $\nabla_{\mathbf{x}_t} \log p(\mathbf{y} | \mathbf{x}_t)$ by resorting to an uninformative prior assumption, whereby an equivalent representation of (1) can be obtained as

$$\mathbf{y} = \mathbf{Q}(\mathbf{A}\mathbf{x}_t + \tilde{\mathbf{n}}_t), \quad (11)$$

where $\tilde{\mathbf{n}}_t \sim \mathcal{N}(\mathbf{0}, \sigma^2 \mathbf{I} + \beta_t^2 \mathbf{A}\mathbf{A}^T)$. As a result, the intractable $p(\mathbf{y} | \mathbf{z}_t = \mathbf{A}\mathbf{x}_t)$ can be asymptotically approximated as the following pseudo-likelihood

$$p(\mathbf{y} | \mathbf{z}_t = \mathbf{A}\mathbf{x}_t) \simeq \tilde{p}(\mathbf{y} | \mathbf{z}_t = \mathbf{A}\mathbf{x}_t) = \int \prod_{m=1}^M \mathbb{1}((z_{t,m} + \tilde{n}_{t,m}) \in \mathbf{Q}^{-1}(y_m)) \mathcal{N}(\tilde{\mathbf{n}}_t; \mathbf{0}, \mathbf{C}_t^{-1}) d\tilde{\mathbf{n}}_t, \quad (12)$$

where $\mathbf{z}_t = \mathbf{A}\mathbf{x}_t$, $\mathbf{C}_t^{-1} = \sigma^2 \mathbf{I} + \beta_t^2 \mathbf{A}\mathbf{A}^T$ and $z_{t,m}, \tilde{n}_{t,m}$ as the m -th elements of $\mathbf{z}_t, \tilde{\mathbf{n}}_t$, respectively, and $\mathbb{1}(\cdot)$ denotes the indicator function, i.e., it equals 1 if the event in the

argument is true and equals 0 otherwise. In particular, if \mathbf{A} is a row-orthogonal matrix such that $\mathbf{A}\mathbf{A}^T$ becomes diagonal, and thus so is the covariance \mathbf{C}_t^{-1} , Meng & Kabashima (2023) derives a closed-form solution of $\nabla_{\mathbf{x}_t} \log p(\mathbf{y} \mid \mathbf{x}_t)$ as Meng & Kabashima (2023). Unfortunately, there is no closed-form solution for general matrices \mathbf{A} , which hinders the application of QCS-SGM to general matrices \mathbf{A} .

3. QCS-SGM+: Improved QCS-SGM for general sensing matrices \mathbf{A}

3.1. A New Perspective

To dress the intrinsic limitation of QCS-SGM (Meng & Kabashima, 2023), we introduce an improved version of it, which we call QCS-SGM+, that can deal with general sensing matrices \mathbf{A} beyond the (approximate) row-orthogonal ones. Our key observation is that obtaining the pseudo-likelihood distribution $\tilde{p}(\mathbf{y} \mid \mathbf{z}_t = \mathbf{Ax}_t)$ (12) can be viewed as computing a partition function of the posterior distribution with respect to (w.r.t.) random variables $\tilde{\mathbf{n}}_t$, where $\mathcal{N}(\tilde{\mathbf{n}}_t; \mathbf{0}, \mathbf{C}_t^{-1})$ acts as a prior distribution and $\prod_{m=1}^M \mathbb{1}((z_{t,m} + \tilde{n}_{t,m}) \in Q^{-1}(y_m))$ as a factorized likelihood distribution. The computation of partition function one of the most fundamental problems in Bayesian inference and various approximate Bayesian methods have been proposed. As a result, while we cannot yield an exact closed-form solution for general (non-diagonal) covariance matrices \mathbf{C}_t^{-1} , we can obtain an estimation of it using efficient approximate inference methods.

3.2. Pseudo-likelihood score via EP

We resort to the well-known expectation propagation (EP) (Minka, 2001) or moment matching (Opper et al., 2005) to approximate the pseudo-likelihood distribution (or partition function) $\tilde{p}(\mathbf{y} \mid \mathbf{z}_t = \mathbf{Ax}_t)$ (12), whereby an efficient approximation of the pseudo-likelihood score $\nabla_{\mathbf{x}_t} \log p(\mathbf{y} \mid \mathbf{x}_t)$ accordingly.

Specifically, we approximate the integral in $\tilde{p}(\mathbf{y} \mid \mathbf{z}_t = \mathbf{Ax}_t)$ (12) in three different ways as follows¹:

$$\begin{aligned} \tilde{p}(\mathbf{y} \mid \mathbf{z}_t = \mathbf{Ax}_t) &\approx \\ &\begin{cases} \int \prod_{m=1}^M \mathbb{1}((z_{t,m} + \tilde{n}_{t,m}) \in Q^{-1}(y_m)) \\ \quad \times \mathcal{N}(\tilde{n}_{t,m}; \frac{h_m^F}{\tau^F}, \frac{1}{\tau^F}) d\tilde{\mathbf{n}}_t & (a) \\ \int \prod_{m=1}^M \mathcal{N}(\tilde{n}_{t,m}; \frac{h_m^G}{\tau^G}, \frac{1}{\tau^G}) \mathcal{N}(\tilde{\mathbf{n}}_t; \mathbf{0}, \mathbf{C}_t^{-1}) d\tilde{\mathbf{n}}_t & (b) \\ \int \prod_{m=1}^M \mathcal{N}(\tilde{n}_{t,m}; \frac{h_m^G}{\tau^G}, \frac{1}{\tau^G}) \mathcal{N}(\tilde{n}_{t,m}; \frac{h_m^F}{\tau^F}, \frac{1}{\tau^F}) d\tilde{\mathbf{n}}_t & (c) \end{cases} \end{aligned} \quad (13)$$

Intuitively, (13-a) approximates the correlated Gaussian

¹The results might differ in a constant scaling factor which is safely ignored as it does not affect the final concerned score function.

$\mathcal{N}(\tilde{\mathbf{n}}_t; \mathbf{0}, \mathbf{C}_t^{-1})$ with a product of independent Gaussians $\prod_{m=1}^M \mathcal{N}(\tilde{n}_{t,m}; \frac{h_m^F}{\tau^F}, \frac{1}{\tau^F})$, (13-b) approximates the non-Gaussian likelihood $\mathbb{1}((z_{t,m} + \tilde{n}_{t,m}) \in Q^{-1}(y_m))$ with a Gaussian likelihood $\mathcal{N}(\tilde{n}_{t,m}; \frac{h_m^G}{\tau^G}, \frac{1}{\tau^G})$, and (13-c) combines the two approximations together. Importantly, in contrast to the original intractable integral in (12) in the case of general matrices, all the three approximations in (13-a) lead to tractable integrals. In particular, the first approximation (13-a) results in a closed-form approximation as follows

$$\tilde{p}(\mathbf{y} \mid \mathbf{z}_t = \mathbf{Ax}_t) \approx \frac{e^{\frac{(h_m^F)^2}{2\tau^F}}}{2} \left[\text{erfc}\left(\frac{-\tilde{u}_{y_m}}{\sqrt{2}}\right) - \text{erfc}\left(\frac{-\tilde{l}_{y_m}}{\sqrt{2}}\right) \right] \quad (14)$$

As a result, it can be calculated that the noise-perturbed pseudo-likelihood score $\nabla_{\mathbf{x}_t} \log p_{\beta_t}(\mathbf{y} \mid \mathbf{x}_t)$ for the quantized measurements \mathbf{y} in (1) can be computed as

$$\nabla_{\mathbf{x}_t} \log p_{\beta_t}(\mathbf{y} \mid \mathbf{x}_t) = \mathbf{A}^T \mathbf{G}(\beta_t, \mathbf{y}, \mathbf{A}, \mathbf{z}_t, \mathbf{h}^F, \tau^F), \quad (15)$$

where $\mathbf{G}(\beta_t, \mathbf{y}, \mathbf{A}, \mathbf{z}_t, \mathbf{h}^F, \tau^F) = [g_1, g_2, \dots, g_M]^T \in \mathbb{R}^{M \times 1}$ with the m -th element being

$$g_m = -\frac{\sqrt{2\tau^F} \left[\exp\left(-\frac{\tilde{u}_{y_m}^2}{2}\right) - \exp\left(-\frac{\tilde{l}_{y_m}^2}{2}\right) \right]}{\sqrt{\pi} \left[\text{erfc}\left(-\frac{\tilde{u}_{y_m}}{\sqrt{2}}\right) - \text{erfc}\left(-\frac{\tilde{l}_{y_m}}{\sqrt{2}}\right) \right]}, \quad (16)$$

where

$$\tilde{u}_{y_m} = -\sqrt{\tau^F} z_{t,m} - \frac{h_m^F}{\sqrt{\tau^F}} + u_{y_m} \sqrt{\tau^F}, \quad (17)$$

$$\tilde{l}_{y_m} = -\sqrt{\tau^F} z_{t,m} - \frac{h_m^F}{\sqrt{\tau^F}} + l_{y_m} \sqrt{\tau^F}. \quad (18)$$

Consequently, the remaining task is to determine the associated parameters $(\mathbf{h}^F, \tau^F, \mathbf{h}^G, \tau^G)$ in (13). To this end, we resort to the moment matching principle of EP (Minka, 2001; Opper et al., 2005) by imposing a consistency of the associated posterior mean $\mathbb{E}[\tilde{n}_{t,m}]$ and variance $\mathbb{V}[\tilde{n}_{t,m}]$ of $\tilde{n}_{t,m}$ from all the three approximations in (13), denoted as (m_m^a, χ^a) , (m_m^b, χ^b) and (m_m^c, χ^c) for (13-a), (13-b), and

(13-c), respectively, which can be computed as follows

$$m_m^a = \frac{h_m^F}{\tau^F} - \frac{2 \exp\left(-\frac{\tilde{u}_{y_m}}{2}\right) - 2 \exp\left(-\frac{\tilde{l}_{y_m}}{2}\right)}{\sqrt{2\pi\tau^F} \left[\operatorname{erfc}\left(-\frac{\tilde{u}_{y_m}}{\sqrt{2}}\right) - \operatorname{erfc}\left(-\frac{\tilde{l}_{y_m}}{\sqrt{2}}\right) \right]}, \quad (19)$$

$$\chi^a = \frac{1}{\tau^F} - \frac{1}{M} \sum_{m=1}^M \left[\frac{2\tilde{u}_{y_m} \exp\left(-\frac{\tilde{u}_{y_m}^2}{2}\right) - 2\tilde{l}_{y_m} \exp\left(-\frac{\tilde{l}_{y_m}^2}{2}\right)}{\sqrt{2\pi\tau^F} \left[\operatorname{erfc}\left(-\frac{\tilde{u}_{y_m}}{\sqrt{2}}\right) - \operatorname{erfc}\left(-\frac{\tilde{l}_{y_m}}{\sqrt{2}}\right) \right]} \right] + \left(m_m^a - \frac{h_m^F}{\tau^F} \right)^2, \quad (20)$$

$$m_m^b = [(\tau^G \mathbf{I} + \mathbf{C}_t)^{-1} \mathbf{h}^G]_m, \quad (21)$$

$$\chi^b = \operatorname{Tr}[(\tau^G \mathbf{I} + \mathbf{C}_t)^{-1}] / M, \quad (22)$$

$$m_m^c = \frac{h_m^G + h_m^F}{\tau^G + \tau^F}, \quad (23)$$

$$\chi^c = \frac{1}{\tau^G + \tau^F}, \quad (24)$$

where $\operatorname{erfc}(z) = \frac{2}{\sqrt{\pi}} \int_{-\infty}^z e^{-t^2} dt$ is the complementary error function (erfc) of the standard normal distribution.

In the special case of 1-bit quantization, i.e., sign measurements as in (5), the results of (m_m^a, χ^a) in (19, 20) and g_m in (16) can be further simplified as follows

$$m_m^a = \frac{h_m^F}{\tau^F} + \frac{2y_m e^{-\frac{\tilde{l}^2}{2}}}{\sqrt{2\pi\tau^F} \operatorname{erfc}\left(\frac{y_m \tilde{l}}{\sqrt{2}}\right)}, \quad (25)$$

$$\chi_m^a = \frac{1}{\tau^F} - \frac{1}{M} \sum_{m=1}^M \left[\left(m_m^a - \frac{h_m^F}{\tau^F} \right)^2 - \frac{2y_m \tilde{l} e^{-\frac{\tilde{l}^2}{2}}}{\sqrt{2\pi\tau^F} \operatorname{erfc}\left(\frac{y_m \tilde{l}}{\sqrt{2}}\right)} \right], \quad (26)$$

$$g_m = \frac{y_m \sqrt{2\tau^F} e^{-\frac{\tilde{l}^2}{2}}}{\sqrt{\pi} \operatorname{erfc}\left(\frac{y_m \tilde{l}}{\sqrt{2}}\right)} \quad (27)$$

$$(28)$$

where $\tilde{l} = -\sqrt{\tau^F} z_{t,m} - \frac{h_m^F}{\sqrt{\tau^F}}$. Subsequently, imposing the following moment-matching conditions, i.e.,

$$m_m^a = m_m^b = m_m^c, \quad (29)$$

$$\chi^a = \chi^b = \chi^c, \quad (30)$$

one can obtain $(\mathbf{h}^F, \tau^F, \mathbf{h}^G, \tau^G)$ iteratively, and hence the targeted pseudo-likelihood score (15) afterwards.

3.3. QCS-SGM+

By combining the pseudo-likelihood score (15) approximated via EP and the prior score from SGM, we readily obtain the improved version of QCS-SGM, dubbed as

QCS-SGM+, using the annealed Langevin dynamics (ALD) (Song & Ermon, 2019), as shown in Algorithm 1.

Algorithm 1 QCS-SGM+

Input: $\{\beta_t\}_{t=1}^T, \epsilon, K, \mathbf{y}, \mathbf{A}, \sigma^2$, quantization codewords \mathcal{Q} and thresholds $\{[l_q, u_q] | q \in \mathcal{Q}\}$

Initialization: $\mathbf{x}_1^0 \sim \mathcal{U}(0, 1)$

for $t = 1$ **to** T **do**

$$\alpha_t \leftarrow \epsilon \beta_t^2 / \beta_T^2$$

for $k = 1$ **to** K **do**

 Draw $\mathbf{z}_t^k \sim \mathcal{N}(\mathbf{0}, \mathbf{I})$

for $it = 1$ **to** $IterEP$ **do**

Initialization: $\mathbf{h}^F, \tau^F, \mathbf{h}^G, \tau^G$

$$\mathbf{h}^G = \frac{m_m^a}{\chi^a} - \mathbf{h}^F$$

$$\tau^G = \frac{1}{\chi^a} - \tau^F$$

$$\mathbf{h}^F = \frac{m_m^b}{\chi^b} - \mathbf{h}^G$$

$$\tau^F = \frac{1}{\chi^b} - \tau^G$$

 Compute $\nabla_{\mathbf{x}_t} \log p_{\beta_t}(\mathbf{y} | \mathbf{x}_t)$ as (15)

$$\mathbf{x}_t^k = \mathbf{x}_t^{k-1} + \alpha_t \left[\mathbf{s}_{\theta}(\mathbf{x}_t^{k-1}, \beta_t) + \nabla_{\mathbf{x}_t} \log p_{\beta_t}(\mathbf{y} | \mathbf{x}_t) \right] + \sqrt{2\alpha_t} \mathbf{z}_t^k$$

Output: $\hat{\mathbf{x}} = \mathbf{x}_T^K$

It is important to note that while it seems from (31, 22) that a matrix inverse $(\tau^G \mathbf{I} + \mathbf{C}_t)^{-1}$ is needed in each iteration every \mathbf{C}_t , this is in fact not necessary since there exists one efficient implementation method using singular value decomposition (SVD) similar to Meng & Kabashima (2022). Specifically, denote $\mathbf{A} = \mathbf{U} \Sigma \mathbf{V}^T$ as the SVD of \mathbf{A} and Σ^2 as the element-wise square of singular values, i.e., diagonal elements of Σ , then after some algebra, it can be shown that the terms involving a matrix inverse can be efficiently computed as follows

$$\begin{aligned} \mathbf{m}^b &= (\tau^G \mathbf{I} + \mathbf{C}_t)^{-1} \mathbf{h}^G, \\ &= \mathbf{U} \operatorname{diag}\left(\frac{\sigma^2 + \beta_t^2 \Sigma^2}{\tau_G(\sigma^2 + \beta_t^2 \Sigma^2) + 1}\right) \mathbf{U}^T \mathbf{h}^G, \\ \chi^b &= \operatorname{Tr}[(\tau^G \mathbf{I} + \mathbf{C}_t)^{-1}] / M \\ &= \operatorname{Tr}\left[\mathbf{U} \operatorname{diag}\left(\frac{\sigma^2 + \beta_t^2 \Sigma^2}{\tau_G(\sigma^2 + \beta_t^2 \Sigma^2) + 1}\right) \mathbf{U}^T\right] / M \\ &= \left\langle \frac{\sigma^2 + \beta_t^2 \Sigma^2}{\tau_G(\sigma^2 + \beta_t^2 \Sigma^2) + 1} \right\rangle \end{aligned} \quad (31)$$

which only needs to replace the values of β_t, τ_G for different iterations. Hence, the main computational burden lies in the SVD of sensing matrix \mathbf{A} , but only one time is required. On the other hand, it is empirically shown that the QCS-SGM+ converges fast with a small number $IterEP$ of EP iterations yields very good results, as demonstrated in Section 4.

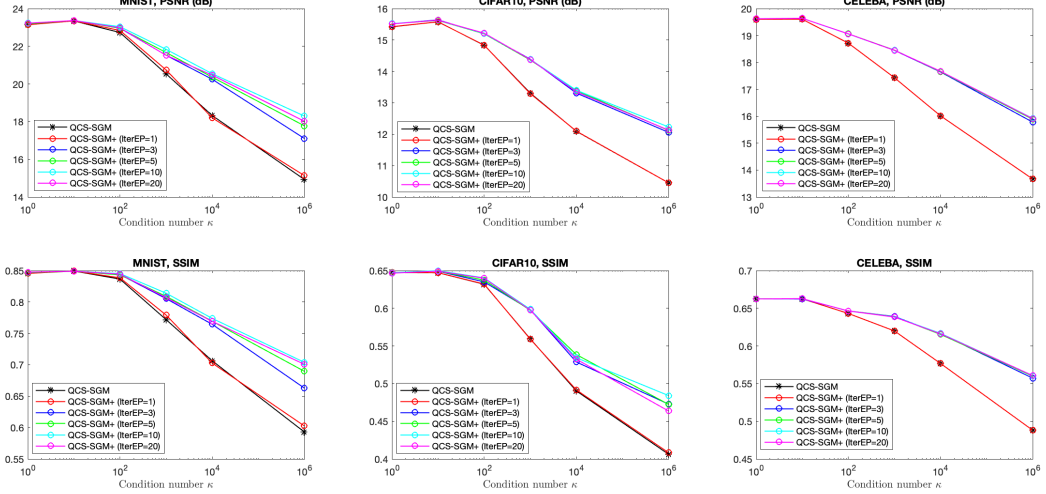


Figure 1. Quantitative comparisons of QCS-SGM+ (proposed) and the original QCS-SGM based on different metrics for 1-bit MNIST, CIFAR10, and CelebA. QCS-SGM+ outperforms QCS-SGM when sensing matrix \mathbf{A} is ill-defined, i.e., with a large condition number.

4. Experiments

In this section, we empirically demonstrate the efficacy of the proposed QCS-SGM+ in various scenarios for general sensing matrices. In particular, similar as Rangan et al. (2019), we consider a broader class of random matrices called right-orthogonally invariant matrices with different condition numbers. When the condition number is 1, it reduces to the i.i.d. Gaussian matrix \mathbf{A} , i.e., $A_{ij} \sim \mathcal{N}(0, 1/M)$ considered in Meng & Kabashima (2023), which is approximately row-orthogonal. However, for larger condition numbers $\gg 1$, it is far from row-orthogonal. Therefore, our main goal is to verify the effectiveness of the proposed QCS-SGM+ for right-orthogonally invariant matrices with large condition numbers.

Datasets: Same as Meng & Kabashima (2023), we consider three popular datasets: MNIST (LeCun & Cortes, 2010), Cifar-10 (Krizhevsky & Hinton, 2009), and CelebA (Liu et al., 2015), and the high-resolution Flickr Faces High Quality (FFHQ) (Karras et al., 2018). MNIST (LeCun & Cortes, 2010) are grayscale images of size 28×28 pixels so that the input dimension for MNIST is $N = 28 \times 28 = 784$ per image. Cifar-10 (Krizhevsky & Hinton, 2009) consists of natural RGB images of size 32×32 pixels, resulting in $N = 32 \times 32 \times 3 = 3072$ inputs per image. For CelebA dataset (Liu et al., 2015), we cropped each face image to a 64×64 RGB image, resulting in $N = 64 \times 64 \times 3 = 12288$ inputs per image. The FFHQ are high-resolution RGB images of size 256×256 , so that $N = 256 \times 256 \times 3 = 196608$ per image. Note that to evaluate the out-of-distribution (OOD) performance, we also cropped FFHQ to

size 64×64 , as OOD samples for CelebA. All images are normalized to range $[0, 1]$.

QCS-SGM+: For fair of comparison, same as QCS-SGM (Meng & Kabashima, 2023), we adopt the NCSNv2 (Song & Ermon, 2020) in all cases. Specifically, for MNIST, we train a NCSNv2 (Song & Ermon, 2020) model on the MNIST training dataset with a similar training set up as Cifar10 in Song & Ermon (2020), while we directly use the for Cifar-10, and CelebA, and FFHQ, which are available in this [Link](#). Therefore, the prior score can be estimated using these pre-trained NCSNv2 models. After observing the quantized measurements as (1), we can infer the original \mathbf{x} by posterior sampling via QCS-SGM+ in Algorithm 1. It is important to note that, *we select images \mathbf{x} that are unseen by the pre-trained SGM models*.

4.1. 1-bit Quantization

In this subsection, we perform experiments on the extremely coarse quantization case, i.e., 1-bit measurements. Specifically, we consider images of the MNIST (LeCun & Cortes, 2010) and CelebA datasets (Liu et al., 2015) in the same setting as Meng & Kabashima (2023). For comparison, apart from QCS-SGM+, we also show results of QCS-SGM (Meng & Kabashima, 2023), BIPG (Liu et al., 2020), and OneShot (Liu & Liu, 2022). For BIPG, and OneShot, we follow the default setting as the open-sourced code of Liu & Liu (2022). For QCS-SGM, we follow exactly the same setting as their open-sourced code (Meng & Kabashima, 2023)

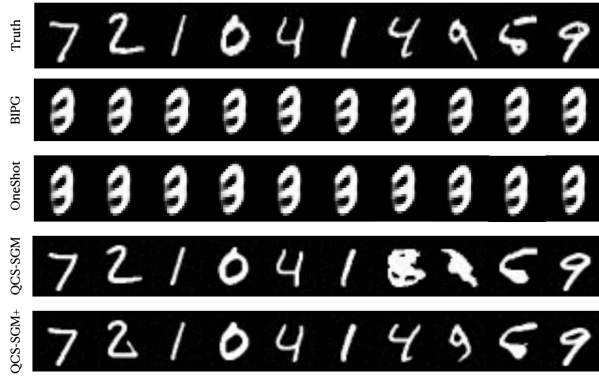
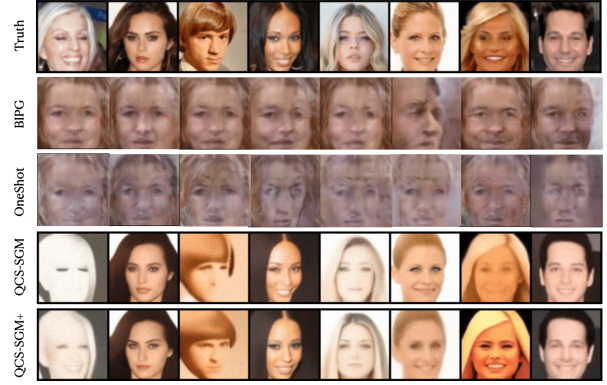
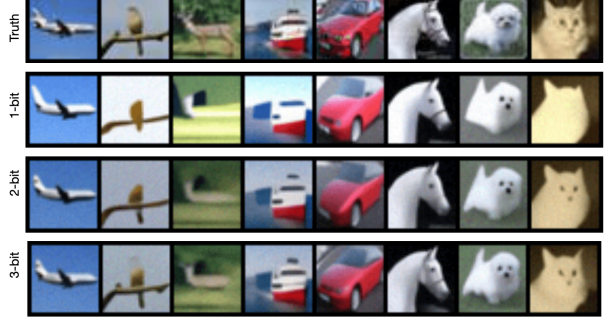

 (a) MNIST, $M = 400, \sigma = 0.05$

 (b) CelebA, $M = 4000, \sigma = 0.001$

Figure 2. Typical reconstructed images from 1-bit measurements on MNIST and CelebA when condition number of \mathbf{A} is 1000. QCS-SGM+ recovers original images from 1-bit measurements even when $M \ll N$. Compared to other methods, QCS-SGM+ recovers more natural images with good perceptual quality and outperforms the original QCS-SGM.



(a) QCS-SGM



(b) QCS-SGM+

Figure 3. Typical reconstructed images on Cifar10 for different number of bits when condition number of \mathbf{A} is 1000. $M = 2000, \sigma = 0.001$

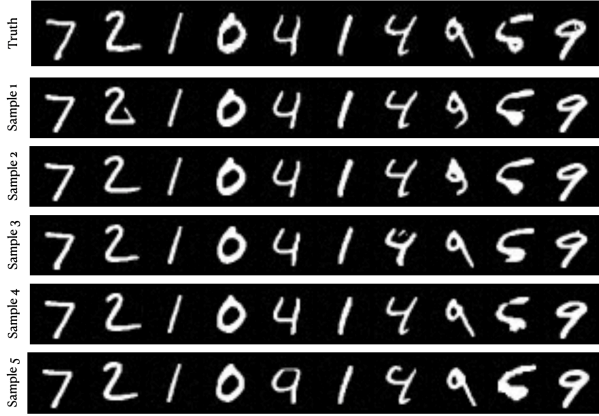
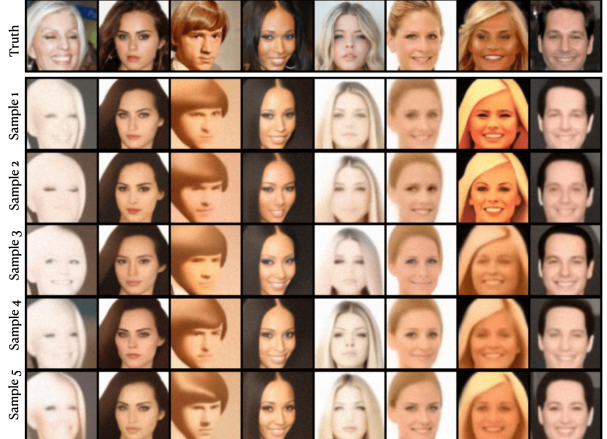

 (a) MNIST, $M = 400, \sigma = 0.05$

 (b) CelebA, $M = 4000, \sigma = 0.001$

Figure 4. Random samples of MNIST and CelebA with different random initializations using QCS-SGM+ when condition number of \mathbf{A} is 1000.

First, we evaluate the convergence performances of the proposed QCS-SGM+ with different numbers of EP iterations and compare them with the original QCS-SGM. The results are shown in Figure 1. It can be seen that QCS-SGM+ converges well for small number of EP iterations on all datasets of MNIST, Cifar10, and CelebA. More importantly, when the condition number of \mathbf{A} is large, QCS-SGM+ apparently outperforms QCS-SGM under different metrics, which demonstrates its advantage and applicability for general matrices. A comparison of QCS-SGM+ and QCS-SGM for different M is shown in Figure 5, which also shows the superiority of QCS-SGM+.

The typical reconstructed images from 1-bit measurements with fixed $M \ll N$ are shown in Figure 2 for both MNIST and CelebA. It can be seen that even when the condition number of 1000 and thus \mathbf{A} is far from row-orthogonal, the QCS-SGM+ can still faithfully recover the images from 1-bit measurements with $M \ll N$ measurements while other methods, including QCS-SGM, might fail or only recover quite vague images.

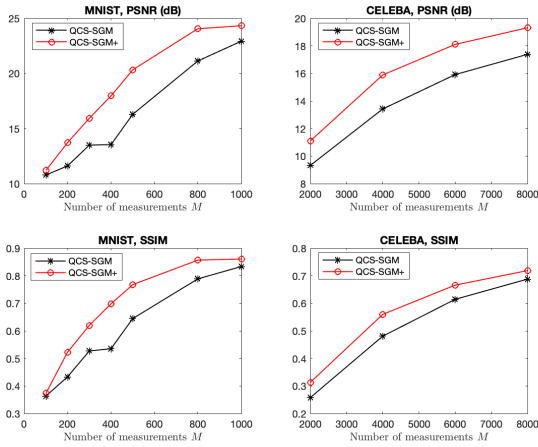


Figure 5. Comparison of QCS-SGM+ with QCS-SGM under different M with fixed condition number 1000 for MNIST and CelebA, respectively.

Multiple samples & Uncertainty Estimates: Same as QCS-SGM, as one kind of sampling method, QCS-SGM+ can yield multiple samples with different random initialization so that we can easily obtain confidence intervals or uncertainty estimates of the reconstructed results, as shown in Figure 4.

4.2. Multi-bit Quantization

Then, we evaluate the efficacy of QCS-SGM+ in the case of multi-bit quantization, e.g., 2-bit, 3-bit. The results on Cifar-10 and CelebA are shown in Figure 3 with a com-

parison with QCS-SGM. As expected, with the increase of quantization resolution, the reconstruction performances get better. For the same number of quantization bit, QCS-SGM+ outperforms QCS-SGM.

5. Conclusion

In this paper, to address the limitation of QCS-SGM to row-orthogonal matrices, we propose an improved version of QCS-SGM called QCS-SGM+. By viewing the likelihood computation as a Bayesian inference problem, QCS-SGM+ efficiently approximates the intractable likelihood score using the well-known expectation propagation (EP) algorithm. To verify the effectiveness of QCS-SGM, we conducted experiments on a variety of baseline datasets, which demonstrate that the proposed QCS-SGM+ outperforms QCS-SGM by a large margin when sensing matrices are far from row-orthogonal. One limitation of QCS-SGM+ is that it requires iterative EP message passing, which is computationally slower than QCS-SGM, although we propose an efficient implementation via SVD. As future work, it is important to further reduce the complexity of QCS-SGM+ or search for other kinds of more efficient alternative methods.

References

- Asim, M., Daniels, M., Leong, O., Ahmed, A., and Hand, P. Invertible generative models for inverse problems: mitigating representation error and dataset bias. In *International Conference on Machine Learning*, pp. 399–409. PMLR, 2020.
- Awasthi, P., Balcan, M.-F., Haghtalab, N., and Zhang, H. Learning and 1-bit compressed sensing under asymmetric noise. In *Conference on Learning Theory*, pp. 152–192. PMLR, 2016.
- Bora, A., Jalal, A., Price, E., and Dimakis, A. G. Compressed sensing using generative models. In *International Conference on Machine Learning*, pp. 537–546. PMLR, 2017.
- Bussi, G. and Parrinello, M. Accurate sampling using langevin dynamics. *Physical Review E*, 75(5):056707, 2007.
- Dai, W. and Milenkovic, O. Information theoretical and algorithmic approaches to quantized compressive sensing. *IEEE transactions on communications*, 59(7):1857–1866, 2011.
- Dhariwal, P. and Nichol, A. Diffusion models beat gans on image synthesis. *Advances in Neural Information Processing Systems*, 34:8780–8794, 2021.

Goodfellow, I., Pouget-Abadie, J., Mirza, M., Xu, B., Warde-Farley, D., Ozair, S., Courville, A., and Bengio, Y. Generative adversarial nets. In Ghahramani, Z., Welling, M., Cortes, C., Lawrence, N., and Weinberger, K. (eds.), *Advances in Neural Information Processing Systems*, volume 27. Curran Associates, Inc., 2014. URL <https://proceedings.neurips.cc/paper/2014/file/5ca3e9b122f61f8f06494c97blafccf3-Paper.pdf>.

Hand, P. and Joshi, B. Global guarantees for blind de-modulation with generative priors. *Advances in Neural Information Processing Systems*, 32, 2019.

Ho, J., Jain, A., and Abbeel, P. Denoising diffusion probabilistic models. *Advances in Neural Information Processing Systems*, 33:6840–6851, 2020.

Hyvärinen, A. Consistency of pseudolikelihood estimation of fully visible boltzmann machines. *Neural Computation*, 18(10):2283–2292, 2006.

Jacques, L., Laska, J. N., Boufounos, P. T., and Baraniuk, R. G. Robust 1-bit compressive sensing via binary stable embeddings of sparse vectors. *IEEE transactions on information theory*, 59(4):2082–2102, 2013.

Jin, K. H., McCann, M. T., Froustey, E., and Unser, M. Deep convolutional neural network for inverse problems in imaging. *IEEE Transactions on Image Processing*, 26(9):4509–4522, 2017.

Jung, H. C., Maly, J., Palzer, L., and Stollenwerk, A. Quantized compressed sensing by rectified linear units. *IEEE transactions on information theory*, 67(6):4125–4149, 2021.

Karras, T., Aila, T., Laine, S., and Lehtinen, J. Progressive growing of gans for improved quality, stability, and variation. In *International Conference on Learning Representations*, 2018.

Kingma, D. P. and Welling, M. Auto-encoding variational bayes. *arXiv preprint arXiv:1312.6114*, 2013.

Kirkpatrick, S., Gelatt Jr, C. D., and Vecchi, M. P. Optimization by simulated annealing. *science*, 220(4598):671–680, 1983.

Krizhevsky, A. and Hinton, G. Learning multiple layers of features from tiny images. Technical report, Citeseer, 2009.

Langley, P. Crafting papers on machine learning. In Langley, P. (ed.), *Proceedings of the 17th International Conference on Machine Learning (ICML 2000)*, pp. 1207–1216, Stanford, CA, 2000. Morgan Kaufmann.

LeCun, Y. and Cortes, C. MNIST handwritten digit database. 2010. URL <http://yann.lecun.com/exdb/mnist/>.

Liu, J. and Liu, Z. Non-iterative recovery from nonlinear observations using generative models. In *Proceedings of the IEEE/CVF Conference on Computer Vision and Pattern Recognition*, pp. 233–243, 2022.

Liu, Z., Luo, P., Wang, X., and Tang, X. Deep learning face attributes in the wild. In *Proceedings of International Conference on Computer Vision (ICCV)*, December 2015.

Liu, Z., Gomes, S., Tiwari, A., and Scarlett, J. Sample complexity bounds for 1-bit compressive sensing and binary stable embeddings with generative priors. In *International Conference on Machine Learning*, pp. 6216–6225. PMLR, 2020.

Meng, X. and Kabashima, Y. Diffusion model based posterior sampling for noisy linear inverse problems. *arXiv preprint arXiv:2211.12343*, 2022.

Meng, X. and Kabashima, Y. Quantized compressed sensing with score-based generative models. In *International Conference on Learning Representations (ICLR)*, 2023.

Meng, X., Wu, S., and Zhu, J. A unified bayesian inference framework for generalized linear models. *IEEE Signal Processing Letters*, 25(3):398–402, 2018.

Minka, T. P. Expectation propagation for approximate bayesian inference. In *Proceedings of the Seventeenth conference on Uncertainty in artificial intelligence*, pp. 362–369, 2001.

Neal, R. M. Annealed importance sampling. *Statistics and computing*, 11(2):125–139, 2001.

Nichol, A. Q. and Dhariwal, P. Improved denoising diffusion probabilistic models. In *International Conference on Machine Learning*, pp. 8162–8171. PMLR, 2021.

Opper, M., Winther, O., and Jordan, M. J. Expectation consistent approximate inference. *Journal of Machine Learning Research*, 6(12), 2005.

Pan, X., Zhan, X., Dai, B., Lin, D., Loy, C. C., and Luo, P. Exploiting deep generative prior for versatile image restoration and manipulation. *IEEE Transactions on Pattern Analysis and Machine Intelligence*, 2021.

Plan, Y. and Vershynin, R. Robust 1-bit compressed sensing and sparse logistic regression: A convex programming approach. *IEEE Transactions on Information Theory*, 59(1):482–494, 2012.

Plan, Y. and Vershynin, R. One-bit compressed sensing by linear programming. *Communications on Pure and Applied Mathematics*, 66(8):1275–1297, 2013.

Radford, A., Metz, L., and Chintala, S. Unsupervised representation learning with deep convolutional generative adversarial networks. *arXiv preprint arXiv:1511.06434*, 2015.

Rangan, S., Schniter, P., and Fletcher, A. K. Vector approximate message passing. *IEEE Transactions on Information Theory*, 65(10):6664–6684, 2019.

Rezende, D. and Mohamed, S. Variational inference with normalizing flows. In *International conference on machine learning*, pp. 1530–1538. PMLR, 2015.

Roberts, G. O. and Tweedie, R. L. Exponential convergence of langevin distributions and their discrete approximations. *Bernoulli*, pp. 341–363, 1996.

Rombach, R., Blattmann, A., Lorenz, D., Esser, P., and Ommer, B. High-resolution image synthesis with latent diffusion models. In *Proceedings of the IEEE/CVF Conference on Computer Vision and Pattern Recognition*, pp. 10684–10695, 2022.

Sohl-Dickstein, J., Weiss, E., Maheswaranathan, N., and Ganguli, S. Deep unsupervised learning using nonequilibrium thermodynamics. In *International Conference on Machine Learning*, pp. 2256–2265. PMLR, 2015.

Song, Y. and Ermon, S. Generative modeling by estimating gradients of the data distribution. *Advances in Neural Information Processing Systems*, 32, 2019.

Song, Y. and Ermon, S. Improved techniques for training score-based generative models. *Advances in neural information processing systems*, 33:12438–12448, 2020.

Turq, P., Lantelme, F., and Friedman, H. L. Brownian dynamics: Its application to ionic solutions. *The Journal of Chemical Physics*, 66(7):3039–3044, 1977.

Vincent, P. A connection between score matching and denoising autoencoders. *Neural computation*, 23(7):1661–1674, 2011.

Welling, M. and Teh, Y. W. Bayesian learning via stochastic gradient langevin dynamics. In *Proceedings of the 28th international conference on machine learning (ICML-11)*, pp. 681–688. Citeseer, 2011.

Xu, Y. and Kabashima, Y. Statistical mechanics approach to 1-bit compressed sensing. *Journal of Statistical Mechanics: Theory and Experiment*, 2013(02):P02041, feb 2013. doi: 10.1088/1742-5468/2013/02/p02041. URL <https://doi.org/10.1088/1742-5468/2013/02/p02041>.

Xu, Y., Kabashima, Y., and Zdeborová, L. Bayesian signal reconstruction for 1-bit compressed sensing. *Journal of Statistical Mechanics: Theory and Experiment*, 2014(11):P11015, nov 2014. doi: 10.1088/1742-5468/2014/11/p11015. URL <https://doi.org/10.1088/1742-5468/2014/11/p11015>.

Zhu, J., Meng, X., Lei, X., and Guo, Q. A unitary transform based generalized approximate message passing. *arXiv preprint arXiv:2210.08861*, 2022.

Zymnis, A., Boyd, S., and Candes, E. Compressed sensing with quantized measurements. *IEEE Signal Processing Letters*, 17(2):149–152, 2009.